

Research Article

Morphological and Molecular Genetic Retrospective Analysis of *KRAS*, *NRAS*, *BRAF*, and MSI (Microsatellite Instability) Pattern in Colorectal Cancer

Flavia Vrenna, Anastasia Nocita, Giuseppina Alberto, Rosanna Patarino and Federico Tallarigo*

Department of Surgical Pathology, Medicine and Oncology, St John of God Hospital, Italy

Abstract

Colorectal cancer is the second most common cancer in both men and women. However colorectal cancer is not a single type of cancer. Its pathogenesis depends on the anatomical location of the tumor and differs from the right side and the left side of the colon. Tumors of the right-sided proximal colon and left-sided distal colon have different molecular and histological features. In right-sided tumors, mutations in the DNA mismatch repair pathway are commonly seen, and these tumors generally have flat histology. Mutations related to the chromosomal instability pathway such as APC, KRAS p53 are seen in left-sided tumors and these tumors demonstrate polypoid morphology. Responses to therapy are totally different among these tumor entities. Patients with left colorectal cancer benefit most from adjuvant chemotherapies such as 5-fluorouracil-based regimens and targeted therapies such as epidermal growth factor receptor therapy and have a better prognosis. Patients with right colorectal cancer do not respond well to conventional chemotherapies but demonstrate more promising results with immunotherapies because these tumors have a high antigenic load. It is essential for the development of effective therapeutic regimens and better treatment options to evaluate right- and left-sided tumors as separate entities and design the therapeutic regimen considering the differences between these two tumors. In the present review, we aimed to compare right and left colorectal cancers in terms of anatomical, histological, epidemiological, molecular and genetic perspectives and discuss the response of these tumors to adjuvant targeted therapy and immunotherapy.

Introduction

Colorectal cancers can be traced back to lifestyles and familiarity. Risk factors are represented, overweight and reduced physical activity, smoking and excess alcohol. Additional risk conditions are Crohn's disease and ulcerative colitis. Hereditary susceptibilities (attributable to syndromes in which genetic mutations have been identified are Familial Adenomatous Polyposis (FAP) and Lynch syndrome. Diagnosis is made by colonoscopy and biopsy for histological examination. The colon is about 150 cm long and extends from ileocecal valve to anus [1]. It is made up of seven parts including cecum, ascending colon, transverse colon, descending colon, sigmoid colon. Right-sided CRC tumors (RCRC) arise from the ascending colon and proximal two-thirds of the colon transverse and left-sided CRC (LCRC) tumors arise from the descending and sigmoid colon and a distal third of the transverse colon [2,3]. In addition to the difference in their origin, these tumors show different histology. While tumors of the left side right-sided show sessile serrated adenomas or mucinous adenocarcinomas, left-sided tumors show tubular, villous,

and tubulovillous adenocarcinomas [4]. Since left-sided tumors have a polypoid morphology, they are easier to detect by colonoscopy in the early stages of carcinogenesis. The right CRC has a flat morphology that is difficult to detect [5,6]. The genomic composition of RCRC and LCRC is totally different from each other. While RCRC patients tend to have more Microsatellite Instability High (MSI-high) tumors, LCRC patients tend to have high Chromosomal Instability (CIN-high) tumors [7,8].

CRC Genetics and Molecular Pathways

Mutations in specific genes can lead to colorectal cancer, as happens in other types of cancer. Such mutations can appear in oncogenes, tumor suppressor genes and DNA repair mechanisms [9]. Pathogenic mechanisms leading to this situation can be included in three different pathways, namely Chromosomal Instability (CIN), Microsatellite Instability (MSI), and CpG island methylator phenotype (CIMP) [10]. The underlying mechanisms of CIN include alterations in chromosome segregation, telomere dysfunction, and DNA damage response, affecting critical genes involved in maintaining proper cellular function, such as *APC*, *KRAS*, *PI3K*, and *TP53*, among others. *APC* and mutations cause translocation of β -catenin into the nucleus and drive transcription of genes implicated in tumorigenesis and invasion, while mutations in *KRAS* and *PI3K* lead to constant activation of MAP kinase, thereby increasing cell proliferation. Finally, loss-of-function mutations in *TP53*, which codes for p53, the major cell cycle checkpoint, cause uncontrolled entry into the cell cycle [11]. The microsatellite instability pathway is caused by a hypermutable phenotype due to loss of DNA repair mechanisms. The ability to repair short DNA chains or tandem repeats (two to five base pair repeats) is impaired in tumors with microsatellite instability; therefore, mutations tend to accumulate in those regions. Loss of expression of Mismatch Repair (MMR) genes

Citation: Vrenna F, Nocita A, Alberto G, Patarino R, Tallarigo F. Morphological and Molecular Genetic Retrospective Analysis of *KRAS*, *NRAS*, *BRAF*, and MSI (Microsatellite Instability) Pattern in Colorectal Cancer. *Ann Clin Case Stud.* 2022; 4(4): 1066.

Copyright: © 2022 Flavia Vrenna

Publisher Name: Medtext Publications LLC

Manuscript compiled: Dec 29th, 2022

***Corresponding author:** Federico Tallarigo, Department of Surgical Pathology, Medicine and Oncology, St. John of God Hospital, Crotona, Italy, E-mail: federicotallarigo@libero.it

can be caused by spontaneous events (promoter hypermethylation) or germline mutations. Genes mutated in tumors with microsatellite instability include *MLH1*, *MSH2*, *MSH6*, *PMS1* and *PMS2* [12]. Epigenetic instability, which is responsible for the CpG island methylator phenotype, is another common feature in CRC. The main feature of CIMP tumors is hypermethylation of oncogene promoters, leading to gene silencing and loss of protein expression. Genetics and epigenetics are not exclusive in colorectal cancer and both cooperate in its development, with multiple methylation events often found in point mutations [13]. An example of the combined effect of genetics and epigenetics in the developmental process of colorectal cancer is the presence of *BRAF* mutations and microsatellite instability in many CIMP tumors [14].

Therapeutic Choices

For localized tumors (stage I-III), resective surgery is indicated. For locally advanced lower-middle rectal tumors, surgery must be preceded by pre-operative long-course chemo-radiotherapy or, in selected cases, by pre-operative short-course radiotherapy. In metastatic tumors (stage IV), the choice of therapy requires the molecular characterization of the surgical specimen or biopsy in order to evaluate the mutational status of RAS (*KRAS*, *NRAS*) and *BRAF* and microsatellite instability [15]. As mentioned earlier, three main alterations are found in CRC, namely Microsatellite Instability (MSI), Chromosomal Instability (CIN), and the CpG Island Methylator Phenotype (CIMP). These alterations produce changes in DNA, RNA, proteins or metabolites, which can be measured in the tumor sample, blood or stool and can therefore be used as biomarkers [16].

Materials and Methods

We constructed a data set that included 85 tissue samples derived from diagnostic biopsy or surgical resection. The samples were subjected to a series of chemical-physical transformations to allow the preparation of the material to be subjected to histological evaluation and molecular analysis. We proceed with the reduction of the samples because in the case of surgical biopsies or surgical pieces it is necessary to take one or more representative fragments of the material under examination which are subsequently placed in special containers called "bioCassettes" for processing. This is to prepare the fixed tissue for paraffin embedding. Paraffin embedding consists in the preparation of a block which encloses the sample to be examined. Once the paraffin block has been created, it continues by preparing sections with a thickness of 3 microns to 6 microns through the use of the microtome. The cut sections are adhered to a slide. The latter are intended for staining in Hematoxylin and Eosin to carry out histological examination from which the diagnosis of Carcinoma is obtained. Furthermore, through the use of a sterile scraper, the tissue sample is taken to process it with the aim of detecting any molecular alterations through a PCR analysis. KIT used ("Diotech pharmacogenetics" Easy PGX) (Figure 1-3).

The Principle of the test envisages the use of 8 0.2 ml test tubes preloaded with everything necessary for carrying out the test in anhydrous format, stable and stored at room temperature and also contains the reagents for DNA extraction from samples Fixed in Formalin and Paraffin-Embedded (FFPE).

The Procedure includes several steps as briefly shown below (Flow Chart 1). As regards microsatellite instability, the EasyPGX ready MSI kit was used, a test for *in vitro* diagnostic use for the determination of microsatellite instability in genomic DNA isolated from tumor tissue (fresh, frozen, fixed in formalin included in paraffin) or blood

KRAS codon 12
<ul style="list-style-type: none"> • G12C (34G>T) • G12R (34G>C) • G12S (34G>A) • G12A (35G>C) • G12D (35G>A) • G12V (35G>T)
non distinguibili tra loro
KRAS codon 13
<ul style="list-style-type: none"> • G13D (38G>A)
KRAS codon 59 (non distinguibili tra loro)
<ul style="list-style-type: none"> • A59T (175G>A) • A59E (176C>A) • A59G (176C>G)
KRAS codon 61 (non distinguibili tra loro)
<ul style="list-style-type: none"> • Q61K (181C>A) • Q61L (182A>T) • Q61R (182A>G) • Q61H (183A>C) • Q61H (183A>T)
KRAS codon 117 (non distinguibili tra loro)
<ul style="list-style-type: none"> • R117E (348A>G) • K117R (350A>G) • K117N (351A>T) • K117N (351A>C)
KRAS codon 146 (non distinguibili tra loro)
<ul style="list-style-type: none"> • A146T (436G>A) • A146P (436G>C) • A146V (437C>T)

Figure 1: PCR analysis 1.

NRAS codons 12-13 (non discriminabili tra loro)	NRAS codons 59-61 (non discriminabili tra loro)
<ul style="list-style-type: none"> • G12S (34G>A) • G12C (34G>T) • G12A (35G>C) • G12D (35G>A) • G12V (35G>T) • G13R (37G>C) • G13D (38G>A) • G13V (38G>T) 	<ul style="list-style-type: none"> • A59T (175G>A) • A59D (176C>A) • Q61H (183A>C) • Q61H (183A>T)
	NRAS codon 61
	<ul style="list-style-type: none"> • Q61K (181C>A) • Q61R (182A>G) • Q61L (182A>T)
	NRAS codon 117 (non discriminabili tra loro)
	<ul style="list-style-type: none"> • K117R (350A>G) • K117N (351G>T) • K117N (351G>C)
	NRAS codon 146 (non discriminabili tra loro)
	<ul style="list-style-type: none"> • A146T (436G>A) • A146V (437C>T)

Figure 2: PCR analysis 2.

BRAF codon 600
<ul style="list-style-type: none"> • V600E (1799T>A)* • V600E_{complex} (1799_1800TG>AA)* • V600K (1798_1799GT>AA) • V600D (1799_1800TG>AT)# • V600R (1798_1799GT>AG)#

Figure 3: PCR analysis 3.

amplified by end-point PCR and subsequent analysis of the targets through the denaturation profile (Table 1) (Flow Chart 2).

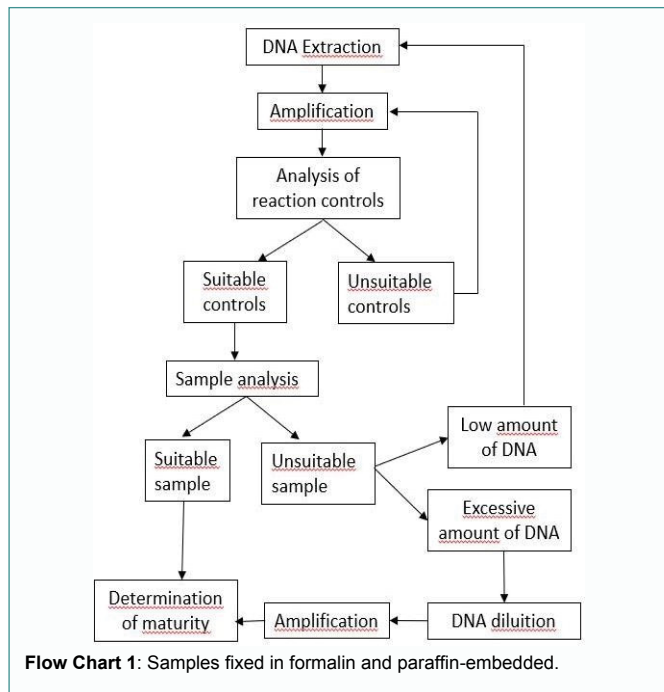
It starts with DNA extraction, then purified DNA, quantification and DNA dilution. Subsequently, a selection and amplification of the DNA regions containing analyzed microsatellites is carried out. Then hybridization of specific labeled probes with the target DNA is performed and the state of instability is determined. Everything is analyzed with the software that returns the denaturation curves.

Results and Discussion

The court of 85 samples was made up of 55 males and 30 females, aged between 35 and 85 (Figure 4). As could be expected, the prevalence fell in the age group greater than 60 years 64; 12 individuals were aged between 40 and 60 years; and only 1 was under the age of 40 (Figure 5).

Table 1: List of Markers Used.

MARCATORE	GENE	NCBI Ref. Seq. (GRCh 38.p12)	CROMOSOMA
BAT25	<i>Ckit</i>	NC_000004.12	4(4q12)
BAT26	<i>MSH</i>	NC_000002.12	2(2p21-p16.3)
NR21	<i>SLC7A8</i>	NC_000014.9	14(14q11.2)
NR22	<i>STT3A</i>	NC_000011.10	11(11q22.2)
NR24	<i>ZNF2</i>	NC_000002.12	2(2q11.1)
NR27	<i>BIRC3</i>	NC_000011.10	11(11q22.2)
CAT25	<i>CASP2</i>	NC_000007.14	7(7q34)
MONO27	<i>MAP4K3</i>	NC_000002.12	2(2p22.1)



Flow Chart 1: Samples fixed in formalin and paraffin-embedded.

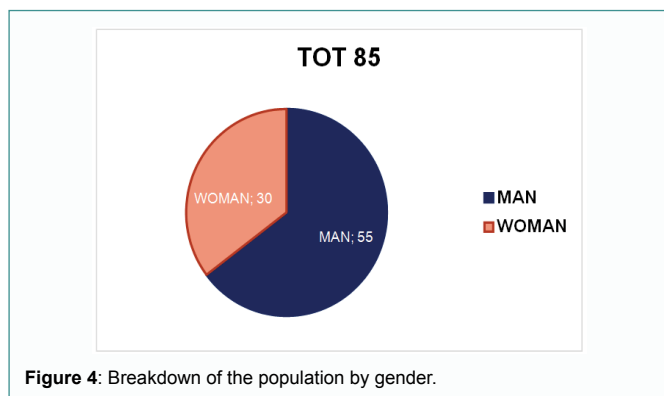
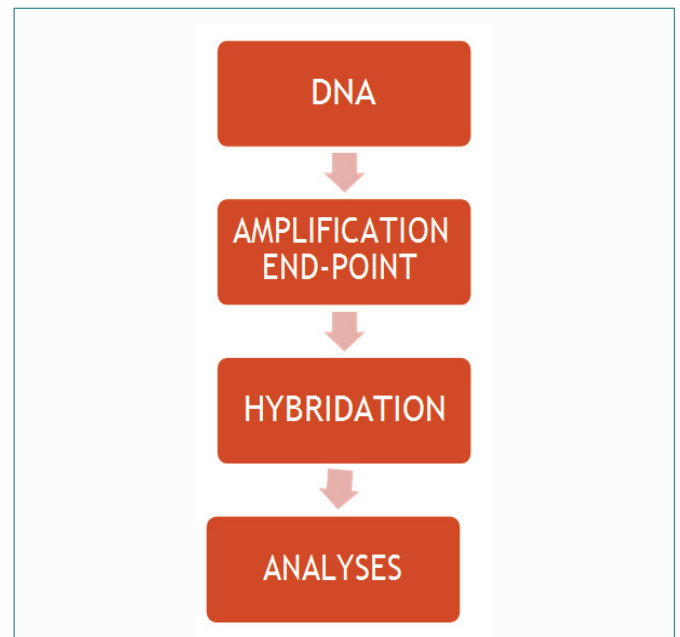


Figure 4: Breakdown of the population by gender.

As regards the anatomical arrangement, we see that as many as 58 tumors came from the left side of the colon, while only 27 cases from the right side of the same (Figure 6). The graph below (Figure 7) summarizes the tumor samples examined.

Taking into consideration also the histological aspect, we noticed that of the 58 samples from the left side of the colon, as many as 54 had a tubulo-villous polypoid histology represented in Figures 8 and 9 and only 4 a mucinous histology (Figure 10 and 11).

In contrast, for samples that originated from the right side of the colon the histotype proportion was the opposite. In fact we see how out of 27 samples 17 had mucinous histotype and 10 polypoid tubulo villous histotype (Figure 12).



Flow Chart 2: Principle of the Procedure.

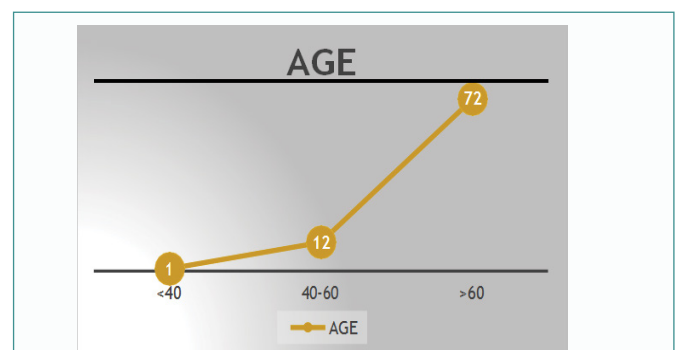


Figure 5: Distribution of cases by age.

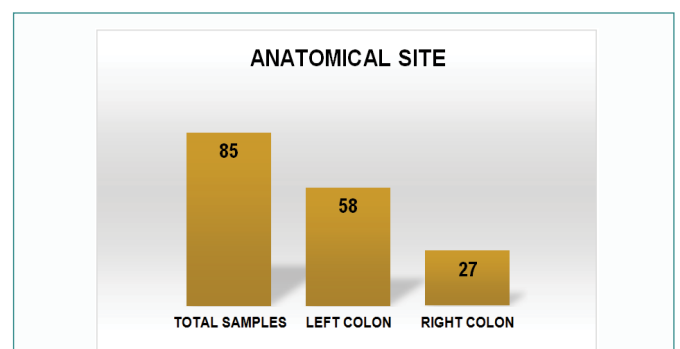


Figure 6: Subdivision of cases by anatomical site.

Having evaluated the macroscopic aspects, we focused on the molecular aspects. The main mutations characterizing the CIN pattern (*KRAS* -*NRAS*) and the MSI pattern (*BRAF*-MSI) were searched for each sample. The mutational analysis involved various catene polymerization reactions (real-time PCR), using the thermal profiles indicated in the specific methods. The samples showing the mutation had a sigmoid trend of the curve. This meant that, in the same way as the control (in green), the sample (in blue) containing the mutated sequence was amplified (Figure 13).

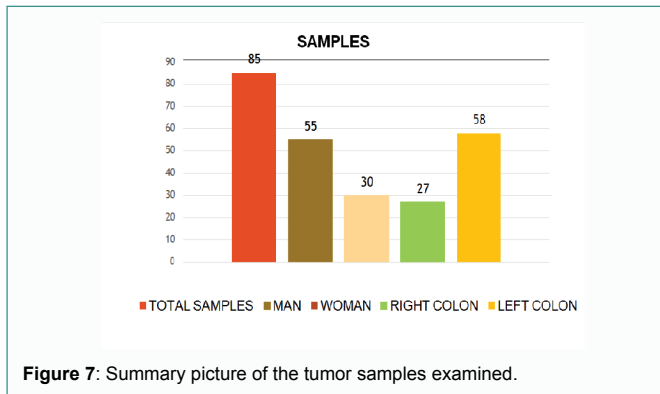


Figure 7: Summary picture of the tumor samples examined.

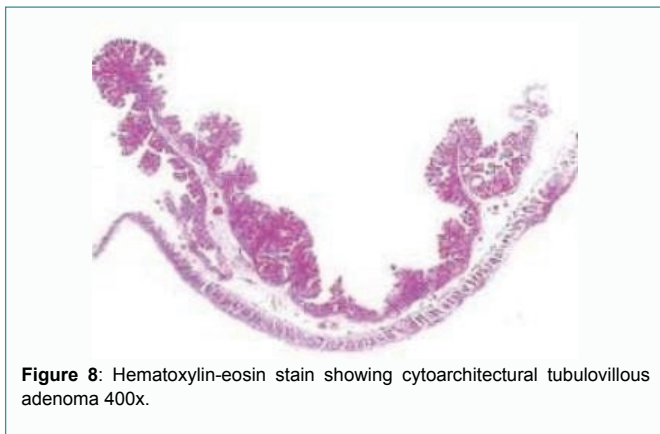


Figure 8: Hematoxylin-eosin stain showing cytoarchitectural tubulovillous adenoma 400x.

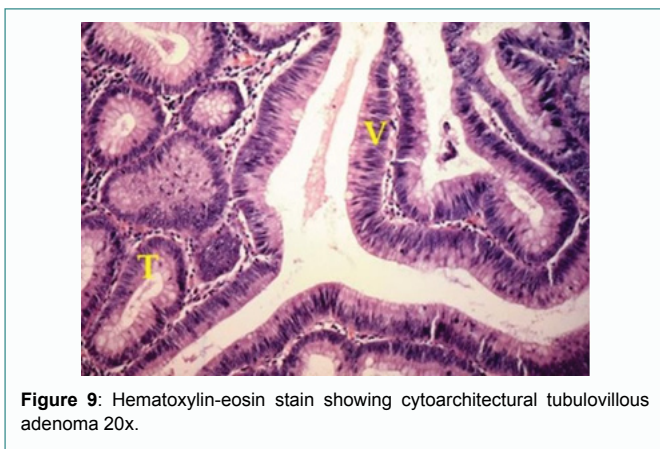


Figure 9: Hematoxylin-eosin stain showing cytoarchitectural tubulovillous adenoma 20x.

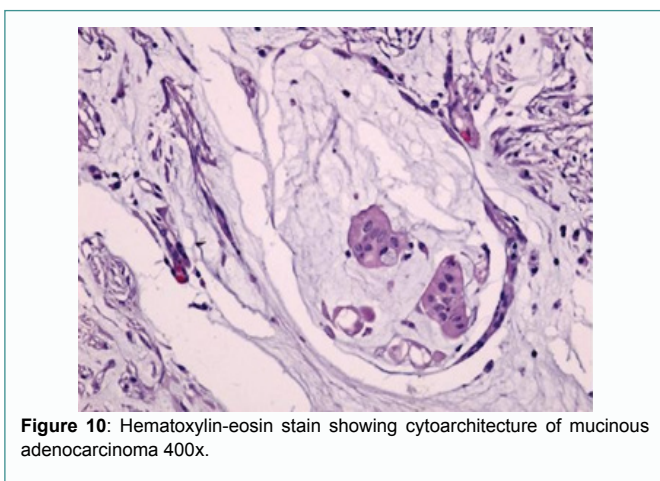


Figure 10: Hematoxylin-eosin stain showing cytoarchitecture of mucinous adenocarcinoma 400x.

Otherwise, demonstrating the lack of mutation, the samples considered wild type were those whose data analysis did not present any amplification (Figure 14).

The results we obtained showed that as many as 51 samples presented at least one mutation (Figure 15) unlike the 34 which did not present any molecular alterations. This underlines how 60% of the samples analyzed had a strong metastatic power.

Focusing on the subgroup of mutants, we found a higher prevalence of mutations belonging to the CIN pattern (45) and only 6 referring to the MSI pattern (Figure 16).

More in detail, as regards the samples relating to the MSI 12% pattern, we found only 2 mutations in the *BRAF* gene corresponding to 4% of all mutations, in which the most mutated amino acid was Valine in position 600 and 4 microsatellite instability positivity corresponding to 8% in relation to the 51 mutations found, two for the bat 25 marker and two for the bat 26 marker (Figure 17).

In parallel, the subgroup of samples presenting mutation of the CIN pattern (K-RAS, N-RAS) was more numerous; in fact we found 45 mutations corresponding to 88% of the total mutations. Furthermore, it is easy to note that there was a higher prevalence of mutations affecting the *KRAS* isoform of the RAS protein rather than the *NRAS* isoform. Those of *KRAS* were 40 (78% of the total mutations) and only 5 of *NRAS* (10% of the total mutations). The most frequent mutation was the one involving codon 12 of the *KRAS* protein, a good 25 cases corresponding to 49% of all the mutations found on *KRAS* and 55% of the mutations of the CIN pattern (K-RAS, N-RAS). This is a very important aspect because it has been seen that mutations of codon 12 are associated with a higher mortality as well as the conversion of Guanine into Thymine (Figure 18).

Having collected all the macroscopic, microscopic and genetic data of the tumor, we put everything in relation. From the analysis of the graphs, a clear distinction emerges clearly between the tumor characteristics in relation to the patient's sex and also in relation to the tumor sites. In the first case, in fact, we can see how within the entire male population (n.55) indicated in yellow (Figure 19), 53 had the tumor lesion on the left side of the colon compared to only 2 on the right side; Furthermore, of these 53, 49 had a tubulo-villous histotype, with relative 42 mutations belonging to the CIN pattern (K-RAS, N-RAS), in particular affecting codons 12 and 13 of K-RAS. At the same time, 25 out of 30 cases of tumor located in the right colon were found in the female population; of which 16 of the mucinous type and only 5 of the tubulo-villous type, with a consequent higher prevalence of the MSI pattern.

Evaluating the same data, taking as reference the population divided according to the site of the tumor, and not according to gender, we can see how the associations with change. First of all, we note how the tumors present on the left side of the colon were more numerous than on the right side, 58 against 27. Furthermore, it should be noted that tubulo-villous histotypes are more frequent on the left side, as well as mucinous histotypes are more present in the right seat. In addition, mutations associated with the CIN pattern (K-RAS, N-RAS) are found to be more frequent than the MSI pattern (*BRAF*, MSI). But the most significant data that emerges is having found a direct correlation between the CIN pattern of chromosomal instability, the tubulo-villous histotype and the left side of the colon, just as in a parallel manner a direct association was found between alterations relating to the MSI, mucinous histotype and right colonic region (Figure 20).

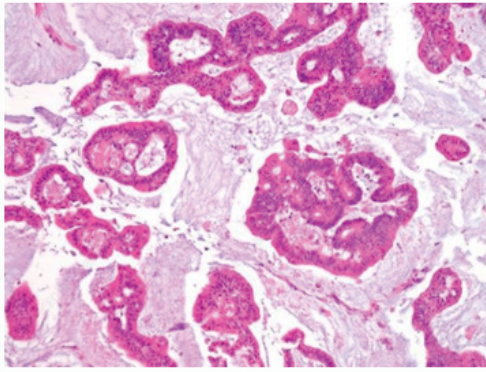


Figure 11: Hematoxylin-eosin stain showing cytoarchitecture of mucinous adenocarcinoma.

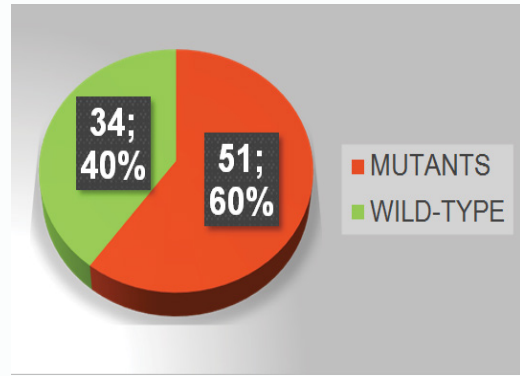


Figure 15: Mutant-wild type ratio.

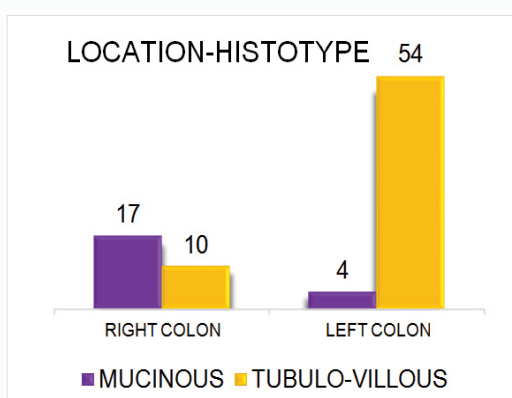


Figure 12: Histogram in relation to the anatomical site-histotype association.

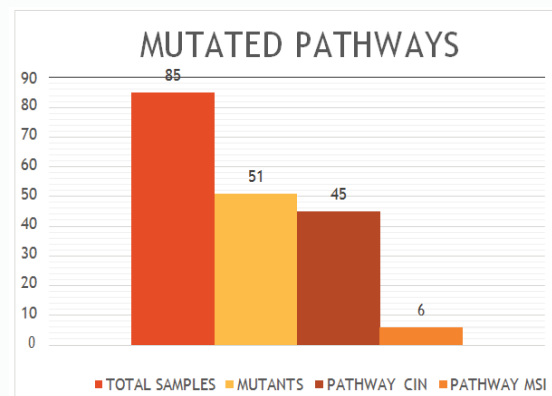


Figure 16: Different incidence of mutations in the analyzed population.

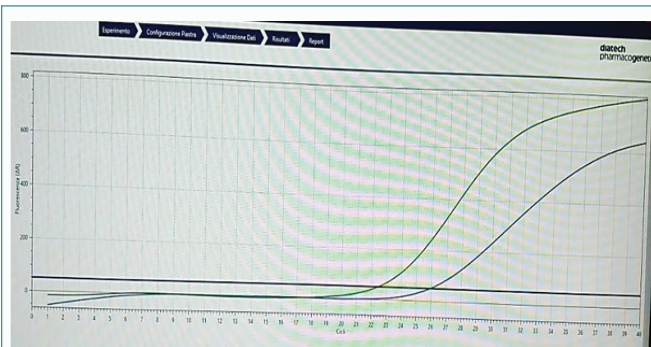


Figure 13: Trend of the amplification curve of a mutated sample.

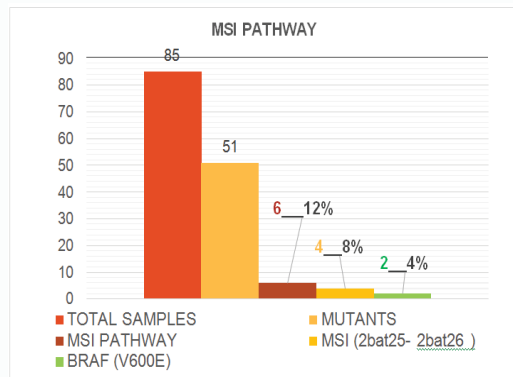


Figure 17: Histogram relating to the prevalence of mutations belonging to the MSI pathway.

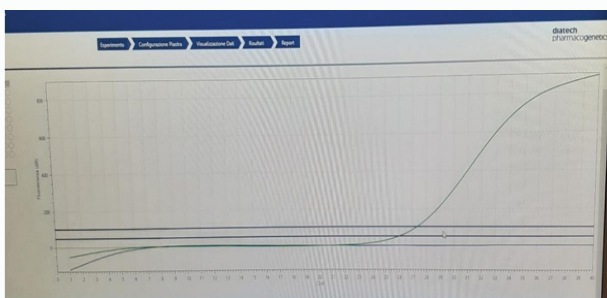


Figure 14: Trend of the amplification curve of a mutated sample.

The results of this investigation aimed at the differential characterization between tumors present in different sites of the colon and the correlation between histotype and molecular profile are currently indispensable both in prognosis and in therapeutic choice.

Conclusion

We collected and analyzed data on various fields relevant to question the term Colorectal Cancer (CRC) and to replace it with Colon Cancer (CC) and Rectal Cancer (RC). Concerning our results, we came to the conclusion to accept CC and RC as different tumor entities in all aspects of experimental and clinical research and to drop the term CRC. Scientists and general practitioners and clinicians

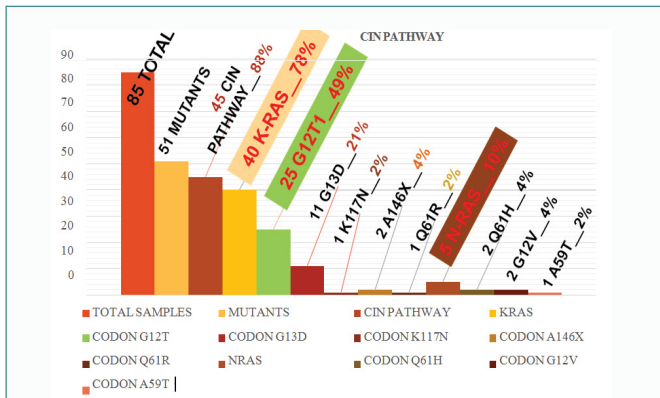


Figure 18: Histogram relating to the prevalence of mutations belonging to the CIN pathway.

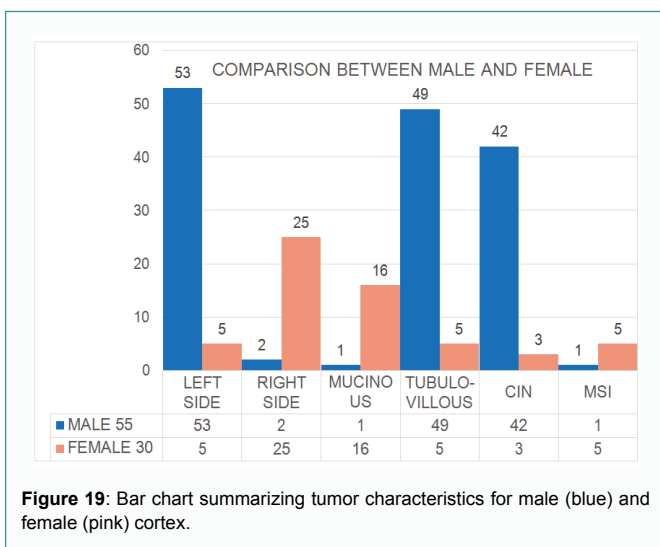


Figure 19: Bar chart summarizing tumor characteristics for male (blue) and female (pink) cortex.

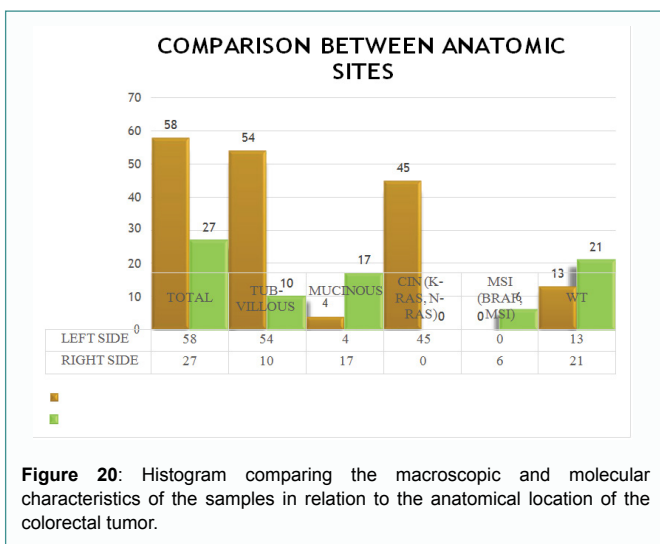


Figure 20: Histogram comparing the macroscopic and molecular characteristics of the samples in relation to the anatomical location of the colorectal tumor.

should respect this change in nomenclature and concentrate on describing the results separately, divided into right and left. These actions will help in the future to improve the accuracy of the results and to improve the individualized treatment of patients with CC and CR [17]. Although early detection of CRC is possible with routine colonoscopic screening, the prevalence is still increasing, especially in

developing countries. Notably, CRC is not one type of disease, but acts like two different diseases in the same organ. The behavior of the CRC is strongly influenced by the anatomical location of the tumor, which in turn influences its molecular and immunological characteristics [18,19]. This also affects the efficacy of the therapies used because currently patients with wild type *KRAS*-type LCRC tumors benefit well from targeted therapies, including anti-EGFR or anti-VEGFR therapies, while patients with RCRC with high MSI seem to benefit more from anti-PDL1 immunotherapies. Therefore, understanding the characteristics of these two different entities is very important for the development of effective therapies. Consequently, although surgical resection is the primary option for all stages and adjuvant therapies appear to be effective in improving survival among patients, there is still a need for more effective therapies both for inoperable mutant *KRAS* (resistant to anti-EGFR therapies) and for wild type tumors that do not present any molecular alteration against which to act.

References

- Gervaz P, Bucher P, Morel P. Two colons-two cancers: paradigm shift and clinical implications. *J Surg Oncol.* 2004;88(4):261-6.
- Iacopetta B. Are there two sides to colorectal cancer? *Int J Cancer.* 2002;101(5):403-8.
- Mik M, Berut M, Dziki L, Trzcinski R, Dziki A. Right and left-sided colon cancer-clinical and pathological differences of the disease entity in one organ. *Arch Med Sci.* 2017;13(1):157-62.
- Marzouk O, Schofield J. Review of histopathological and molecular prognostic features in colorectal cancer. *Cancers (Basel).* 2011;3(2):2767-810.
- Gualco G, Reissenweber N, Cliche I, Bacchi CE. Flat elevated lesions of the colon and rectum: a spectrum of neoplastic and nonneoplastic entities. *Ann Diagn Pathol.* 2006;10(6):333-8.
- Nawa T, Kato J, Kawamoto H, Okada H, Yamamoto H, Kohno H, Endo H, et al. Differences between right- and left-sided colon cancer in patient characteristics, cancer morphology and histology. *J Gastroenterol Hepatol.* 2008;23(3):418-23.
- Glebov OK, Rodriguez LM, Nakahara K, Jenkins J, Cliatt J, Humbyrd CJ, et al. Distinguishing right from left colon by the pattern of gene expression. *Cancer Epidemiol Biomarkers Prev.* 2003;12(8):755-62.
- Carethers JM. One colon lumen but two organs. *Gastroenterology.* 2011;141(2):411-2.
- Fearon ER, Vogelstein B. A genetic model for colorectal tumorigenesis. *Cell.* 1990;61(5):759-67.
- Grady WM, Carethers JM. Genomic and epigenetic instability in colorectal cancer pathogenesis. *Gastroenterology.* 2008;135(4):1079-99.
- Pino MS, Chung DC. The chromosomal instability pathway in colon cancer. *Gastroenterology.* 2010;138(6):2059-72.
- Boland CR, Goel A. Microsatellite instability in colorectal cancer. *Gastroenterology.* 2010;138(6):2073-87.e3.
- Lao VV, Grady WM. Epigenetics and colorectal cancer. *Nat Rev Gastroenterol Hepatol.* 2011;8(12):686-700.
- Weisenberger DJ, Siegmund KD, Campan M, Young J, Long TI, Faasse MA, et al. CpG island methylator phenotype underlies sporadic microsatellite instability and is tightly associated with BRAF mutation in colorectal cancer. *Nat Genet.* 2006;38(7):787-93.
- Carmine P. *Oncologia.* Comprehensive Cancer Centre, AUSL-IRCCS di Reggio Emilia. 2021.
- Ludwig JA, Weinstein JN. Biomarkers in cancer staging, prognosis and treatment selection. *Nat Rev Cancer.* 2005;5(11):845-56.
- Paschke S, Jafarov S, Staib L, Kreuser ED, Maulbecker-Armstrong C, Roitman M, et al. Are colon and rectal cancer two different tumor entities? A proposal to abandon the term colorectal cancer. *Int J Mol Sci.* 2018;19(9):2577.

18. Gervaz P, Bucher P, Morel P. Two colons-two cancers: paradigm shift and clinical implications. *J Surg Oncol.* 2004;88(4):261-6.
19. Hansen IO, Jess P. Possible better long-term survival in left versus right-sided colon cancer- a systematic review. *Dan Med J.* 2012;59(6):A4444.